

The Calculation of 3D High-Frequency Electromagnetic Fields During Induction Heating Using the BEM

A. Mühlbauer, A. Muižnieks and H.-J. Leßmann

Institute for Electroheat, University of Hanover,
Wilhelm-Busch-Str.4, D-3000 Hannover, Germany

Abstract - In the present work a numerical 3D-calculation method for the simulation of the electromagnetic (EM) field for different applications of high-frequency induction heating is developed. The calculation program uses the boundary element method (BEM) and runs on an efficient personal computer (PC). The set-up to be considered is divided into groups of bodies with specific material properties which allow the formulation of simplified conditional equations for the electric vector potential at the surfaces of the set-up components. Finally, some examples of numerically calculated high-frequency current distributions indicate the efficiency of the program developed.

I. GENERAL CONSIDERATIONS

The use of induction heating at high frequency for industrial purposes allows the workpiece to be heated without contact. The distribution of the heat sources in the workpiece should be controlled to get the temperature distribution desired. Because of the highly complicated structure of the electromagnetic field, this requires mathematical modelling of the induction heating process. The complicated geometry of industrial set-ups, in most cases 3D, leads to very high demand on computing resources. Nevertheless, considering the specific properties of high-frequency currents, it is possible to use an effective method for the calculation based on the BEM. By this way, many important problems can be solved using only an efficient PC.

When the range of frequency f between 10 kHz and some MHz is taken into account, the EM penetration depth [1], [2] $\delta = (\pi \cdot f \cdot \sigma \cdot \mu_0 \cdot \mu_r)^{-1/2}$ is of the order of one mm or less. σ is the electric conductivity, μ_0 the permeability of free space and μ_r the relative permeability. In deeper layers of the material, the current and the magnetic flux density vanish. Because the dimensions of the induction heating set-ups are up to some hundred mm, the above-mentioned situation permits us to assume that the currents flow tangentially to the surfaces and the evaluation of the current distribution can be reduced to the calculation of the surface current density \mathbf{j} . Because of the solenoidality of the current

$$\text{div } \mathbf{j} = 0, \quad \text{rot } \mathbf{T} = \mathbf{j} \quad (1a, 1b)$$

the electric vector potential \mathbf{T} [3] is introduced (1b). The divergence and the curl are defined only on the surface S , i.e. in the coordinates η, ξ (Fig. 1). \mathbf{T} corresponds to a vector $\mathbf{T} = (0, 0, T_n)$ with only the normal component T_n not equal to zero. In general, \mathbf{T} is unknown and has to be calculated.

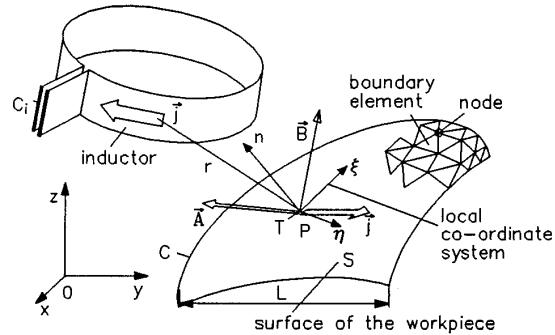


Fig. 1. Set-up of the inductor and the work-piece with fields and co-ordinate systems.

The surface current density \mathbf{j} on the surfaces of the set-up components determines the magnetic vector potential \mathbf{A} at a point P corresponding to Biot-Savart's law. Connected with the relation $\mathbf{B} = \text{rot } \mathbf{A}$ between the magnetic flux density \mathbf{B} and \mathbf{A} this allows us to evaluate the normal component B_n of the magnetic flux density by means of \mathbf{T} :

$$B_n = \frac{\mu_0}{4\pi} \cdot \text{rot}_n \int_S \frac{\text{rot } \mathbf{T}}{r} ds \quad (2)$$

where rot_n is the normal component of the curl. On the surface S of a set-up component, in many cases the conditions for B_n are determined by specific properties of the material. In the following sections equations are set up which consider the situation at the surface of certain materials. Combined with equation (2) for each group of materials, an equation for the electric vector potential \mathbf{T} is obtained. Because of the assumed harmonic time dependency, every quantity may be complex. The numerical method works with non-dimensional equations, and therefore several characteristic quantities are used for standardization. For lengths it is the characteristic length L , and for surface current densities the inductor current I referred to

L is introduced. The vector potential is normalized by the factor $\mu_0 \cdot I / (4\pi)$, the magnetic flux density by the factor $\mu_0 \cdot I / (4\pi \cdot L)$.

Taking (1b) into consideration, the conditions for the surface current density \mathbf{j} result in the boundary conditions for T . Usually it is impossible for the induced current to leave the surface of the arrangement component. Therefore the condition $\mathbf{j} \cdot \mathbf{n} = 0$ is applied at the boundaries of the components. This means a constant value for T at the boundary C of the surface S (Fig. 1). At the feed-in terminals C_i of the inductor, T is set to describe a given distribution of the surface current density.

II. CONDUCTING NON-FERROMAGNETIC BODIES

Set-up components which are both conducting and non-ferromagnetic [4] can be inductors as well as workpieces to be heated. In the material, beyond the EM skin layer, all the components of the magnetic flux density \mathbf{B} , especially the normal component B_n , vanish. According to how high frequency is, there will only be a thin skin layer and the EM flux in the skin layer can be neglected. Taking into consideration the solenoidality of \mathbf{B} , $B_n = 0$ results at the surface S_c of the conducting non-ferromagnetic body. Combining this with (2) the conditional equation of the electric vector potential T is obtained:

$$\text{rot}_n \left(\int_{S_o} \frac{\text{rot} T}{r} ds + \int_{S_c} \frac{\text{rot} T}{r} ds \right) = 0 \quad (3)$$

Equation (3) has to be fulfilled at every point of the surface S_c . S_o means all surfaces of other components where T has to be taken into account.

III. NON-CONDUCTING FERRITE BODIES

Ferrite bodies are frequently used to control the distribution of heat sources. Their field-carrying nature enables us to achieve a certain concentration of the EM field and thus to produce the required distribution of the current. Under industrial conditions, the relative permeability μ_r of ferrite materials ranges from 100 to 10,000. Moreover, its value depends on the temperature and the magnetic field strength as well. If these dependencies have to be considered when calculating 3D EM fields, the amount of computing resources required will become very high. However, in many cases, especially when the magnetic circuits are open, the simplified calculation using the assumption $\mu_r \rightarrow \infty$ leads to results of sufficient precision.

The assumption $\mu_r \rightarrow \infty$ means that the tangential components of \mathbf{B} vanish at the surface of the ferrite, i.e. $B_n = B_t = 0$. Taking into consideration the solenoidality of the magnetic field formulated in the local

co-ordinate system (η, ξ, n) (Fig. 1), $\partial B_n / \partial n = 0$ follows at a plane surface S_F of the ferrite. Applying this to (2), the conditional equation for T is obtained:

$$\frac{\partial}{\partial n} \left[\text{rot}_n \left(\int_{S_o} \frac{\text{rot} T}{r} ds + \int_{S_F} \frac{\text{rot} T}{r} ds \right) \right] = 0 \quad (4)$$

At the surface of the ferrite body, T describes a fictitious surface current which influences the EM-field in the same way as the infinite permeability does.

IV. THIN CONDUCTING STRIPS

The heating of thin strips by the transverse flux coil is one of the recent applications of induction heating [5]. Generally, the gauge of a strip h is small compared with the penetration depth δ as well as compared with the dimensions of the set-up to be considered. In this case the magnetic field will penetrate the strip [6]. Due to the small gauge of the strip, in the strip the magnetic flux tangential to the surface of the strip is insignificant in comparison with the incident field. This means that on both sides of the strip B_n is of the same magnitude. Inside the strip this component B_n induces eddy currents which flow tangentially to the surface.

The small value of h leads to the assumption of a homogeneous current distribution across the gauge of the strip, so that it is sufficient to calculate the surface current \mathbf{j} only [7]. The relation between T and the electric field strength \mathbf{E} , $\text{rot} T = \mathbf{E} \cdot \boldsymbol{\sigma} \cdot h$, combined with the law of induction $\text{rot} \mathbf{E} = -i \cdot \omega \cdot \mathbf{B}$ gives rise to

$$\text{rot}_n \text{rot} T = -i \cdot \omega \cdot h \cdot \boldsymbol{\sigma} \cdot B_n \quad (5)$$

where i denotes the imaginary number and ω the radian frequency. Taking (2) into consideration, the desired non-dimensional conditional equation

$$\text{rot}_n \text{rot} T = -i \cdot \omega_s \text{rot}_n \left(\int_{S_o} \frac{\text{rot} T}{r} ds + \int_{S_s} \frac{\text{rot} T}{r} ds \right), \quad \omega_s = \frac{\mu_0 \cdot \omega \cdot \boldsymbol{\sigma} \cdot h \cdot L}{4\pi} \quad (6)$$

for the calculation of T at the surface S_s of the thin strip is obtained. ω_s denotes the non-dimensional frequency normalized by the characteristic length L .

V. CONDUCTING FERROMAGNETIC BODIES

Due to the high value of the relative permeability μ_r , the magnetic flux tangential to the surface inside the conducting ferromagnetic body may be large and thus should not be neglected. Nevertheless, the small penetration depth δ allows us to use the exponential solution for the EM field inside the skin layer. Assuming a constant value for μ_r , the relation

$$\Phi' = \frac{1}{2} \cdot (1-i) \cdot \delta \cdot \mu_0 \cdot \mu_r \cdot j \times \vec{n} \quad (7)$$

between j on the surface S_{CF} of the conducting ferro-magnetic body and the surface flux density ϕ' can be given. Allowing for the solenoidality of the EM field, (7) gives rise to the relation

$$B_n = -\frac{1}{2} \cdot (1-i) \cdot \delta \cdot \mu_0 \cdot \mu_r \cdot \text{rot}_n \text{rot} T \quad (8)$$

at the surface S_{CF} . Finally, (2) is used to formulate the non-dimensional conditional equation for the calculation of the complex electric vector potential T at S_{CF} :

$$\text{rot}_n \text{rot} T = -(1+i) \cdot \omega_{CF} \cdot \text{rot}_n \left(\int_{S_0} \frac{\text{rot} T}{r} ds + \int_{S_{CF}} \frac{\text{rot} T}{r} ds \right), \quad (9)$$

$$\omega_{CF} = \frac{L}{4 \cdot \pi \cdot \delta \cdot \mu_r}$$

where ω_{CF} denotes the non-dimensional frequency.

VI. TOTAL SET-UP

The groups of bodies with different properties above described form the total set-up to be considered. The distribution of T is calculated on the overall surface $S = S_C + S_F + S_S + S_{CF}$. Each single surface has to belong to one component group. At every surface S_C , S_F , S_S and S_{CF} the attached equation (3), (4), (6) and (9) is considered, where S_0 denotes the remaining surface $S - S_C$, $S - S_F$, $S - S_S$ and $S - S_{CF}$.

VII. NUMERICAL PROCEDURE

For the numerical solution of the problem, the boundary element method (BEM) is used. All the surfaces of the set-up components are divided into finite triangles. The unknown quantity, the vector potential T , is defined at the corners of the triangles and is interpolated in a linear manner inside the triangles. Each triangle k has its local co-ordinate system (η, ξ) (Fig. 2). According to (1b), T and the components of j are connected by (10) in each element k .

$$j_\eta = \frac{T_3 - T_1}{\eta_3}, \quad j_\xi = \frac{T_2 - T_1}{\xi_2} + \frac{T_1 - T_3}{\xi_2 \cdot \eta_3} \cdot \eta_2 \quad (10)$$

The components j_η and j_ξ are transformed to the global co-ordinate system (x, y, z) .

According to Biot-Savart's law the sum

$$A(P) \approx \sum_{k=1}^N \frac{j^k}{r^{P,k}} \cdot S_\Delta^k \quad (11)$$

is used to approximate the magnetic vector potential A in a point P numerically. N denotes the quantity of all

elements, k and S_Δ^k the number and the content of the surface of the element respectively and $r^{P,k}$ the distance between P and the centre of k (Fig. 2). If P is located in k , the corresponding part of the sum is calculated analytically. $\text{rot}_n A$ is described by

$$\text{rot}_n A = \frac{1}{S_\Delta L_\Delta} \oint A dl \approx \frac{1}{S_\Delta} \sum_{i=1}^{\Delta} \frac{A_1^i + A_2^i}{2} \cdot l_i \quad (12)$$

where Δ is the number of elements which have the node M and S_Δ is the content of the hatched surface in Fig. 3. The operator $\text{rot}_n \text{rot} T = \text{rot} j$ is replaced by a line integral (Fig. 3) and approximated numerically by a sum similar to (12). The discretization of the partial derivative of B_n (Fig. 4) uses

$$\frac{\partial B_n}{\partial n} \approx \frac{1}{S_\Delta} \cdot \frac{\partial}{\partial n} \oint A dl \approx \frac{1}{S_\Delta} \sum_{i=1}^{\Delta} \left[\frac{\partial A}{\partial n}(P_i) \cdot l_i + A(P_i) \cdot \frac{\partial l_i}{\partial n} \right] \quad (13)$$

Finally, the numerical sum for the calculation of the partial derivative of $A(P)$ is given by

$$\frac{\partial A}{\partial n}(P) \approx \frac{1}{a} \cdot \sum_{k=1, k \neq i}^N j_k \cdot \left(\frac{1}{r^{P,k}} - \frac{1}{r^{k,P}} \right) + 2 \cdot \pi \cdot j_i \quad (14)$$

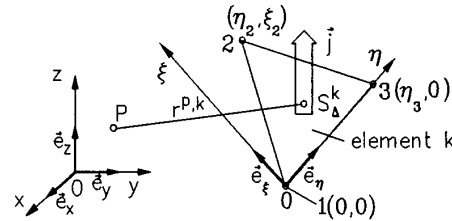


Fig. 2. Boundary element in the local and in the global co-ordinate system.

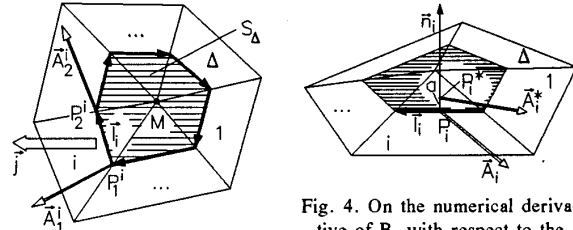


Fig. 3. Numerical line integral round a node M .

Fig. 4. On the numerical derivative of B_n with respect to the component n .

After all the operators in (3), (4), (6) and (9) have been described numerically, the conditional equation at every node can be considered. In this way a system of algebraic equations is obtained. The numerical solution of this system gives the distribution of T in the nodes on the surfaces of the set-up under consideration. Proceeding from T , the distribution of the heat sources is calculated by using the exponential solution for the EM field inside the workpieces.

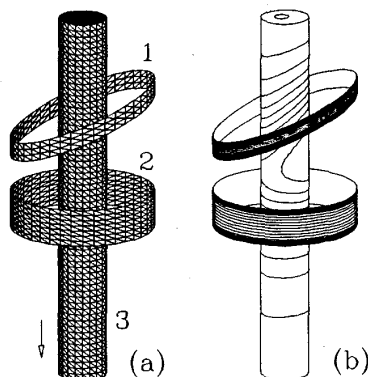


Fig. 5. Influence of non-axisymmetric elements (two inductors (1,2) in antiphase) on the falling jet of the melt (3) during jet-casting (frequency 70 kHz, diameter of the titanium jet 20 mm) discretization (a); calculated current lines (b).

Then, several integral quantities are evaluated, for example the total power, the induced voltage and the inductance and the active resistance of the inductor.

VIII. CALCULATION PROGRAM

The preprocessing uses a programmable commercial CAD-program for PC to display the 3D geometry of the set-up. The triangular boundary elements are drawn as 3D surfaces. An applications program library has been developed for the automatic generation of certain surfaces. The main program builds up the matrix, which describes the algebraic equation system. Gaussian elimination is used as the solution method. Proceeding from the distribution of T , the program calculates the above-mentioned integral quantities. The postprocessing program evaluates the location of the isolines (current lines) of the normal component of T .

IX. EXAMPLES OF NUMERICAL RESULTS

The current lines at the surfaces are taken into account for graphic presentation as a characteristic quantity of the 3D EM field (Fig. 5, Fig. 6). The density of the current lines describes the intensity, and the direction corresponds to that of the current. If T is complex (Fig. 6), the real component as well as the imaginary component is plotted.

CONCLUSIONS

The 3D computer program developed allows us to consider many industrial set-ups in the field of high-frequency induction heating. The physical fundamentals of the high-frequency EM field connected with the specific advantages of the BEM, lead to a simulation program which runs on an efficient personal computer.

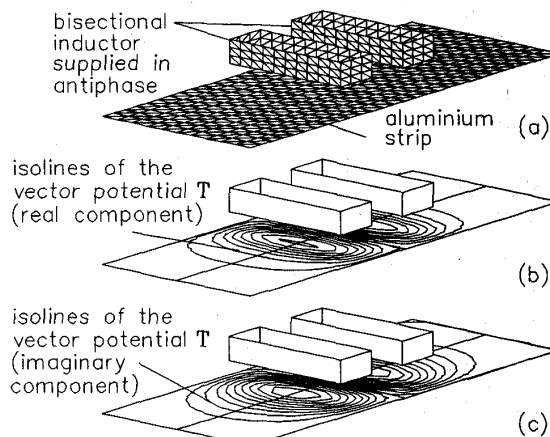


Fig. 6. Induction strip heating by the transverse flux coil: $f = 10$ kHz, gauge of the strip 0.2 mm, width 500 mm; discretization (a); current lines in the strip (b), (c).

REFERENCES

- [1] S.R.H. Hoole and C.J. Carpenter, "Surface impedance models for corners and slots," *IEEE Trans. Magn.*, vol. 21, pp. 1841-1843, 1985.
- [2] S.R.H. Hoole, "Computer Aided Analysis and Design of Electromagnetic Devices," Elsevier, NY, 1989.
- [3] C.J. Carpenter and E.A. Wyatt, "Efficiency of Numerical Techniques for Computing Eddy Currents in Two and Three Dimensions," *Proc. COMPUMAG*, pp. 242-250, Oxford, 1976.
- [4] A. Mühlbauer *et al.*, "Berechnung des dreidimensionalen Hochfrequenzfeldes beim Zonenschmelzen von Silizium," *Archiv für Elektrotechnik*, 76 (1992).
- [5] U.I.E. Induction Heating working group, "Induction Heating - Industrial Applications," U.I.E. 1992.
- [6] H. Tsuboi and K. Kunisue, "Eddy current analysis of thin plates taking account of the source current distributions and its experimental verifications," *IEEE Trans. Magn.*, vol. 27, pp. 4020-4023, 1991.
- [7] A. Mühlbauer *et al.*, "Mathematische 3D-Modellierung des elektromagnetischen und des thermischen Feldes bei der Quersfeld-erwärmung dünner Bleche," in *37.IWK Ilmenau, Germany, 1992*.

A. Mühlbauer was born in Bad Wörishofen, Germany, in 1932. He obtained his Dipl.-Ing. degree in Electrical Engineering from the Technical University of Munich, Germany, and his Ph.D. degree from the Technical University of Hanover, Germany. He worked for Siemens AG for many years and has written over 75 publications in the fields of high-purity silicon, induction heating and melting and other subjects. Since 1979 he has been Director of the Institute for Electroheat and Professor of Electrical Engineering at the University of Hanover, Germany. His main research interests are process modelling, electroheat technology and solar energy conversion.

A. Muižnieks was born in Cēsis, Latvia, in 1961. He obtained his Ph.D. degree in Physics and Mathematics from the Latvia University, Riga, Latvia, in 1991. He is presently research assistant with the Institute for Electroheat at the University of Hanover, Germany.

H.-J. Leßmann was born in Hamburg, Germany, in 1963. He obtained his Dipl.-Ing. degree in Electrical Engineering from the University of Hanover, Germany. Since 1989 he is research assistant with the Institute for Electroheat, University of Hanover, Germany.